Local atomic structure in strained interfaces of $In_xGa_{1-x}As/InP$ heterostructures

F. Boscherini*
Istituto Nazionale di Fisica Nucleare, Laboratori Nazionali di Frascati, P.O. Box 13, I-00044 Frascati (Rome), Italy

C. Lamberti
Dipartimento di Chimica Inorganica, Fisica e dei Materiali, Università di Torino, via P. Giuria 7, I-10125 Torino, Italy

S. Pascarelli†
Istituto Nazionale per la Fisica della Materia, c/o GILDA CRG, ESRF, BP 220, F-38043, Grenoble, France

C. Rigo
CSELT, via G. Reiss Romoli 274, I-10148 Torino, Italy

S. Mobilio
Dipartimento di Fisica, Università di Roma Tre, via della Vasca Navale 84, I-00146 Rome, Italy
and Istituto Nazionale di Fisica Nucleare, Laboratori Nazionali di Frascati, P.O. Box 13, I-00044 Frascati (Rome), Italy
(Received 7 May 1998)

We present a structural study of the interfaces between $In_xGa_{1-x}As$ and InP (and vice versa) by x-ray absorption fine structure spectroscopy (XAFS); the samples investigated are a set of nominally matched $In_xGa_{1-x}As/InP$ short-period superlattices. We find that the coordination numbers around As and Ga deviate significantly from those expected in an abrupt superlattice structure even if interface bonds are taken into account; this demonstrates the presence of unwanted interface layers between InP and In_xGa_xAs (and vice versa). Based on the growth sequence employed and on indications from other techniques, we model the structure as composed of the two nominal layers plus $InAs_xP_{1-x}$ and $In_{0.53}Ga_{0.47}As_{1-y}P_y$ strained interface layers. XAFS is a chemically sensitive probe of the local structure in these strained layers. We find that each bond length measured (As-In, Ga-As, and Ga-P) has a different value, with small variations among the different samples. This implies the presence of structural distortions that accommodate strain at the local level. We find good agreement between the XAFS results and high-resolution x-ray diffraction data that probe the structure in an average way. The results are discussed also with reference to the problem of the band offsets at $In_xGa_{1-x}As/InP$ heterojunctions and to theoretical simulations. [S0163-1829(98)05539-8]

I. INTRODUCTION

$In_xGa_{1-x}As/InP(001)$ heterostructures are widely used in modern optoelectronic devices. From a fundamental point of view this system is studied intensely both theoretically and experimentally as an example of an isovalent, polar junction.[1] There are peculiar features of this heterostructure that affect the electronic structure and optoelectronic response in a fundamental way. If nonlattice-matched structures are grown ($x \neq 0.53$), and provided the $In_xGa_{1-x}As$ layer is sufficiently thin, pseudomorphic growth will result and strain will have a direct effect on the band structure of the ternary layer; the effect of strain can be predicted, for example, within a ''model solid'' approach.[2,3] The changes in the electronic structure of the ternary layer will be reflected in variations of the band offsets (BO's) with the InP; the BO's are the quantities that are of most importance from an applicative point of view and are currently the subject of considerable theoretical and experimental investigation.

Even if the composition $x=0.53$ is used for $In_xGa_{1-x}As$ (at this composition the alloy will be indicated in the following as InGaAs) the atomic composition of the layers has consequences on the strain at the interfaces. In fact, there are no common anions nor common cations in the heterojunction (for the cations this is true because In is different from the average cation of InGaAs, which can be indicated by $\langle In_{0.53}Ga_{0.47}\rangle$, with obvious meaning). This implies that, even if abrupt interfaces are assumed, local strain will be present at the heterojunction.[4,5] We note that the just-quoted papers take the fundamental parameter describing strain to be the variation of the (001) lattice parameter, which is related to the next-nearest-neighbor distance. This point of view arises naturally within diffraction investigations since this technique measures precisely the distance between lattice planes, averaging out local distortions between the planes themselves: the virtual crystal approximation[6,7] (VCA) is thus implied. As such, this picture is a simplification of the real structure as it does not address the value of the individual bond lengths. The effect of the adjustment of the lattice parameter to the value dictated by local composition on the BO's is nonnegligible and has been estimated by *ab initio* methods[8] to be 60 meV for an ideal interface, which is an appreciable fraction of the valence BO of ~ 0.35 eV.

The properties of any real semiconductor heterostructure depend in a crucial way on the growth method and procedure and on the presence of interdiffusion processes at the interfaces. For chemical beam epitaxy (CBE) and metal-organic chemical vapor deposition (MOCVD) grown heterostruc-

TABLE I. Sample growth characteristics: nominal InGaAs and InP thicknesses, number of periods (N), period (P), average perpendicular lattice mismatch ($\langle \Delta a_\perp / a \rangle$), and the four times relevant to the switches between InP and InGaAs growth and vice versa.

Sample	Code	t_{nom}(InP) (Å)	t_{nom}(InGaAs) (Å)	N	P (Å)	$\langle \Delta a_\perp / a \rangle$ (%)	t_1 (s)	t_2 (s)	t_3 (s)	t_4 (s)
1	161	30	30	20	59	0.58	1	1	1	5
2	384	20	20	20	39	0.49	1	1	1	1
3	380	20	20	20	37	-0.14	5	1	10	10
4	411	18	13	65	31	0.48	1	0	1	1
5	406	18	13	65	28	0.87	1	0	1	1

tures it has been suggested that undesired strained layers a few monolayers (ML's) thick are present at both the InP-to-InGaAs and at the InGaAs-to-InP interfaces.[9–11] The composition and thickness (and hence the *strain*) of these interface layers critically affect the band alignment in the interface region[12,13] and evidently modify the potential in which charge carriers move in a device. It is well known that the performance of any real device is influenced by the quality of the interface.[14,15] Interface imperfections such as planarity and compositional grading problems[16] cause scattering processes yielding a reduction of the exciton decay time,[17] a limitation of the electron mobility,[18,19] and an increase of nonradiative recombination.[20] In a superlattice structure both InP-to-InGaAs and InGaAs-to-InP interfaces are present; unwanted interface layers cause the BO's at the two interfaces to be asymmetric, as has been detected experimentally by photoemission spectroscopy.[21] Recently,[22] the presence of these interface layers has been necessary to interpret magneto-photoluminescence measurements of InGaAsP/InP multiquantum barriers, a system closely related to the one presently investigated. In summary, it is clear that a characterization of the interfaces between InP and InGaAs (and vice versa) has a wide range of fundamental and applicative interest.

With the aim of clarifying the atomic structure of InGaAs-InP interfaces at the local scale we have performed an x-ray absorption fine structure (XAFS) investigation at the Ga and As K edges of a set of five nominally lattice-matched InGaAs/InP short-period superlattices (SPSL); we also report a comparison with high-resolution x-ray diffraction (HRXRD) data. There is a twofold interest in SPSL's. Firstly, as the period decreases the relative importance of the interface layers increases and hence it becomes possible to use volume-sensitive probes such as x rays to study their structure. While specific growth sequences are necessary to optimize the properties of SPSL's, compared to longer period structures, the nature of the interfacial layers is expected to be similar and thus our results are of a general validity. Secondly, the system is interesting per se, and finds applications for example in Wannier-Stark modulators.[23] We find that the coordination numbers (CN's) around As and Ga deviate significantly from those expected in an abrupt superlattice (SL) structure even if interface bonds are taken into account and relate this finding to the presence of strained layers at the interfaces. Comparison of the thickness and composition of these layers deduced from XAFS with HRXRD determination of the average strain and period is favorable. We find that each bond length measured (As-In, Ga-As, and Ga-P) has a different value, with small variations among the different samples. This implies the presence of local structural distortions, in a clear illustration of the violation of the VCA in $In_xGa_{1-x}As/InP(001)$ heterostructures; these results will be discussed in the framework of recent findings on related systems.[24–35]

II. SAMPLE DEPOSITION AND EXPERIMENTAL RESULTS

Sample 1 was deposited by MOCVD (Ref. 36). Specific planarization (t_1 and t_3) and switching (t_2 and t_4) times were used in changing from the growth of InP to that of InGaAs (t_1 and t_2) and vice versa (t_3 and t_4). Planarization times refer to the exposure of the just-grown surface with the same group-V precursor, while switching times refer to the exposure to the group-V precursor of the next layer. Only for Sample 1 a $1s$ exposure to H_2 flux was performed between the exposures to the group-V precursors. Samples 2 to 5 were deposited by CBE on InP(001) with similar growth sequences, the only difference being that no exposure to H_2 flux was performed. Growth-related characteristics of our samples are listed in Table I. A detailed description of the growth apparata has already been reported.[11,23]

The experimental period (P) and average perpendicular lattice mismatch ($\langle \Delta a_\perp / a \rangle$) were measured by HRXRD on the ''D2AM'' (BM2) beamline of the European Synchrotron Radiation Facility (ESRF, Grenoble, France). A wavelength of 1 Å (selected by a double crystal Si(111) monochromator) was used in a vertical scattering geometry; the sample and the NaI(Tl) scintillator detector were mounted on a four-circle diffractometer. Harmonics were rejected with a grazing incidence mirror. Since the diffracted intensity varies by many orders of magnitude in going from the substrate to the high-order superlattice peaks and due to the intensity of the ESRF beam the total angular range measured was split in a number of smaller regions with provision of some overlap; each region was then measured by attenuating the beam with an appropriate thickness of Al filters in order to bring the intensity within the range of linearity of the detector. We show in Figs. 1(a) and 1(b) the diffraction pattern in the neighborhood of the (004) reflection for Sample 3, in an extended and restricted L range, respectively. The reflections are labelled with the reciprocal lattice indices *(H, K, L)* of the InP substrate. An example of the total diffraction pattern for

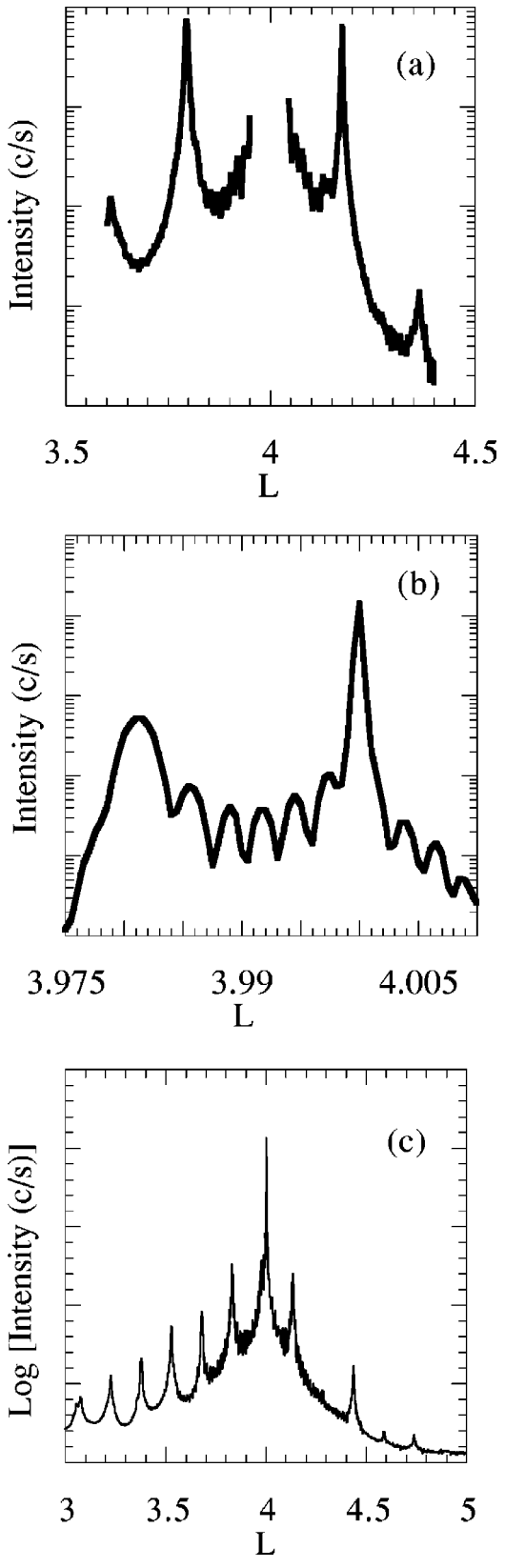

FIG. 1. HRXRD patterns in the neighborhood of the (004) reflection. (a) and (b) refer to Sample 4. In (a) the central region has been omitted and the ± 1 and ± 2 superlattice peaks are evident; in (b) the substrate and 0-order superlattice peak are detected. In (c) we report the full diffraction pattern for Sample 1 in an extended L range, obtained by joining several scans and appropriately renormalizing. The reflections are labelled with the reciprocal lattice indices *(H, K, L)* of the InP substrate.

Sample 1, obtained by joining the different angular regions and appropriately renormalizing, is reported in Fig. 1(c). The absence of the $+2$ superlattice peak is due to the particular thickness, number, and composition of the layers constituting the SL structure. A detailed analysis of diffraction profile in the full angular range within the context of dynamical diffraction theory will be presented elsewhere;[37] here the diffraction patterns will be used to obtain the quantities P and $\langle \Delta a_\perp / a \rangle$.

It is clear from Fig. 1(b) that a non-negligible lattice mismatch is present and a similar behavior was found for all samples. In Table I we list values of period and average perpendicular lattice mismatch obtained from HRXRD for all samples; we note that $\langle \Delta a_\perp / a \rangle$ is negative only for Sample 3.

XAFS measurements were performed in the fluorescence mode at the Ga and As K edges at the ''GILDA'' (BM8) beamline of the ESRF using a dynamically sagittally focussing monochromator[38] with Si(113) crystals. Harmonics were rejected with two grazing incidence mirrors and fluorescence detection was accomplished with a single-element hyper-pure Ge detector. In order to avoid dead-time corrections the total count rate on the detector was limited to 20 000 c/s and a shaping time of 0.25 μm was used on the amplifier. Good signal-to-noise ratio was obtained by integrating between 20 and 50 s/point. The polarization vector of the photon beam was directed along the (011) direction. In the unstrained zinc-blende structure; the polarization factor $3\,\Sigma \cos^2\theta$ (with θ the angle between the bond and the polarization unit vectors, and the sum being over all bonds) averages out to 4 for the first shell, as for a powder sample; for small tetragonal distortions such as those encountered here this is still an excellent approximation. The incident flux was monitored using an Ar-filled ionization chamber. As standards, samples of GaP, InAs, and GaAs were measured in the transmission mode, while a 0.3 mm-thick, unstrained, InGaAs sample deposited on InP was measured in the fluorescence mode. All spectra were measured at room temperature.

Data analysis was performed according to standard procedures.[39,40] The pre-edge and the atomic absorption background were simulated with a linear function and a cubic spline, respectively. The XAFS signals were normalized using the function $J \times [1 - \frac{8}{3}(E - E_0)/E_0]$, where J and E_0 are the discontinuity of the absorption spectrum and the energy corresponding to the maximum derivative at the absorption edge. In Figs. 2(a) and 2(b), we show the background-subtracted raw data at the Ga and As edges. In Figs. 3(a) and 3(b), we report the magnitudes of the Fourier transforms of the k^2-weighted XAFS signal obtained in the range 2.6 to 13 Å^{-1} using a Hanning window function. It is clear that the line shapes, and thus the total XAFS signal, are dominated by the first-shell signal, which appears in the range 1.5–3 Å. The weakness of the second- and third-shell signals is due to the presence of numerous contributions due to different atomic correlations in the various atomic layers, as will be apparent from our discussion of the first-shell signal below; each of these contributions contributes with a different phase shift and the net result is a negligible signal.

It is useful at this point to qualitatively discuss the main features of the spectra based on an analysis of Figs. 3(a) and

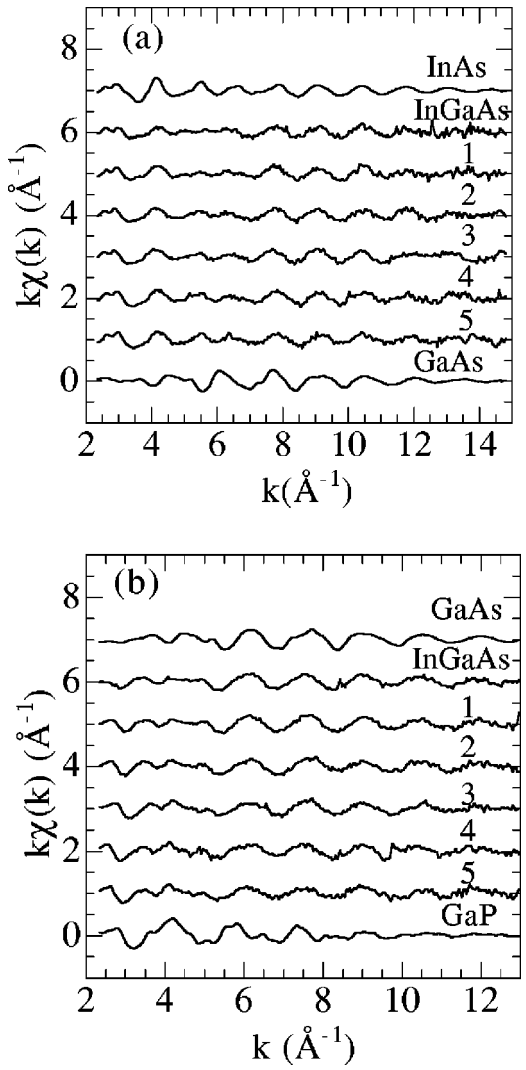

FIG. 2. Background-subtracted raw data at the As (a) and Ga edges (b). Spectra have been offset for graphical purposes.

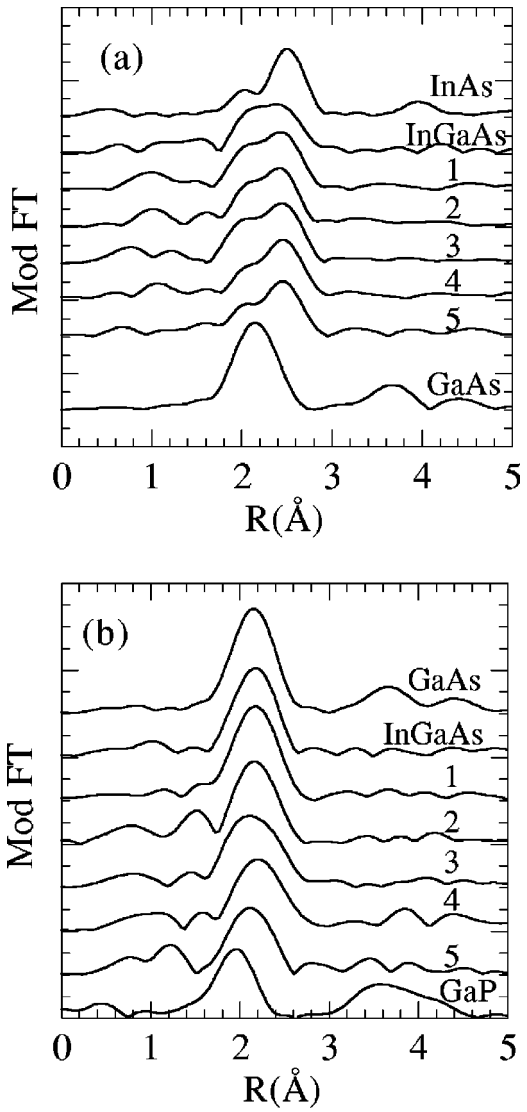

FIG. 3. Magnitudes of the Fourier transform at the As edge (a) and Ga edge (b). Spectra have been offset for graphical purposes.

3(b). At the As edge, Fig. 3(a), the spectrum of the InGaAs standard appears to be a linear combination of the spectrum of InAs and GaAs, with roughly equal weight; this is reasonable as in InGaAs the As-Ga and As-In first-shell coordination numbers (CN's) are expected to be 1.88 and 2.12, respectively. Significantly, however, the spectra of all samples are different from those of InGaAs and inspection of the line shapes suggests a first-shell environment with an excess of In atoms. As for the Ga edge, the spectra of all samples apparently resemble closely that of InGaAs (and of GaAs, which has identical first-shell environment); we note however that Sample 3 has a first-shell peak that is broadened towards lower distances; comparison with the GaP spectrum suggests the presence of some Ga-P correlations.

Quantitative analysis was performed by fitting in k space. An inverse FT was performed in the range 1.6 to 3 Å in order to isolate the first-shell signal. In a SL with abrupt interfaces and in the limit of infinite period Ga atoms are surrounded exclusively by As and As atoms are surrounded by In and Ga with CN's of 2.12 and 1.88, as described above. However, any attempt to fit the Ga signal exclusively with As nearest neighbors failed (except for Sample 1) and it was necessary to include a contribution of P atoms. This is illustrated in Fig. 4 where we show, for Sample 3, in (a) the best fit obtained without P contribution while in (b) the fit using a linear combination of Ga-P and Ga-As contributions, obtained as described in the next paragraph; it is clear that without the Ga-P contribution the fit is completely unable to reproduce the experimental line shape in the low-k region, precisely where it is expected that a light atom such as P will give the strongest contribution.

Each first-shell signal was fitted using a nonlinear least-squares routine. The Ga spectra were fitted with Ga-P and Ga-As contributions, as described, while the As spectra were fitted with a combination of As-Ga and As-In signals. Experimental amplitudes and phases were used. The maximum number of free parameters is $2\Delta k\Delta R/\pi \approx 9$. For the Ga edge, seven free parameters were used: two distances, relative value of the two CN's (the sum being fixed to four), two values of mean-square-relative displacement and two energy-origin shifts. For the As edge, six free parameters were used, the Ga-As distance being fixed to the value found at the Ga edge. The quality of the fits obtained is illustrated in Fig. 4, top panel. In Table II we list the As-In and Ga-P CN's thus

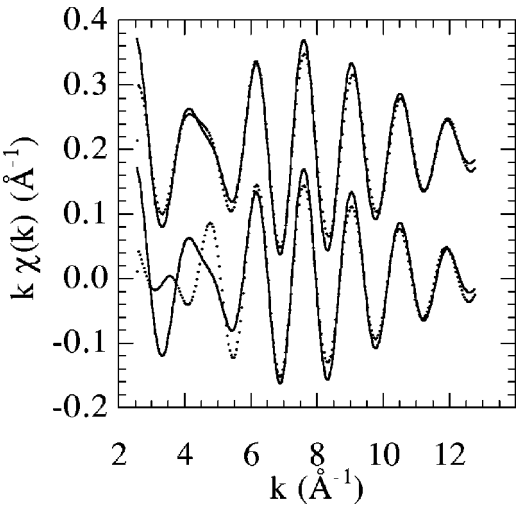

FIG. 4. Comparison of first shell fits for the Ga edge spectra of Sample 3 without (bottom) and with (top) Ga-P contribution; the experimental curve is reported as the continuous line while the fit is the dotted line. The top curve has been offset for graphical purposes.

found; As-Ga and Ga-As CN's can be found by subtraction from 4. Apart from the presence of a significant number of Ga-P bonds it is also clear that the As-In CN's deviate significantly from 2.12, a clear evidence of the deviation of the structure from ideality. Also listed are the nominal thicknesses of InP and InGaAs expressed in ML's (T_1 and T_2, the period being $P=T_1+T_2$). The values of the Ga-As, As-In and Ga-P bond lengths found are listed in Table III. The determination of the Ga-P bond length is affected by a relatively large error, due to the weakness of the signal. It is obvious that each bond length measured has a specific value (with small variations among the various samples). This is a clear illustration of the violation of the VCA in this system and will be discussed in the next section making reference to studies of local structure in similar systems.[24–35] Finally, the values of mean-square-relative displacements were found identical to those in standard compounds, and thus will not be discussed further.

III. DISCUSSION

We have already discussed the fact that the experimental CN's are not compatible with those expected for a SL with abrupt interfaces and infinite period. As the period decreases the relative importance of interface bonds between the InP and InGaAs layers increases and this results in an increase of the Ga-P and As-In CN's. In fact, assuming each layer to be composed of an integral number of (electrically neutral) ML's the following relations can be deduced (see the Appendix):

$$N_{ai}(\text{Ga-P})=\frac{2}{T_2}, \tag{1}$$

$$N_{ai}(\text{As-In})=\frac{2.12\times[T_2-1]+3.06}{T_2}. \tag{2}$$

Here the subscript ''ai'' refers to ''abrupt interfaces.'' These values can become non-negligible when the nominal layer thicknesses are a few ML's, as in our case. A structure with abrupt interfaces was proposed by Vandenberg *et al.*[5] in their

TABLE II. Nominal thicknesses of InP and InGaAs layers (T_1 and T_2), As-In and Ga-P CN's, excess of the As-In and Ga-P CN's with respect to the abrupt interface case, values of n'(InAsP) and n'(InGaAsP) and minimum values of x and y.

Sample	Code	T_1 (ML)	T_2 (ML)	N(As-In)	N(Ga-P)	δ(As-In)	δ(Ga-P)	n'(InAsP) (ML)	n'(InGaAsP) (ML)	x_{min}	y_{min}
				±0.2	±0.2	±0.2	±0.2	±1	±0.3		
1	161	10.2	10.2	2.6	0	0.4	-0.2	3.5	0	0.34	
2	384	6.8	6.8	2.7	0.8	0.4	0.5	2.4	1.4	0.35	0.21
3	380	6.8	6.8	2.8	1.4	0.5	1.1	2.5	2.4	0.37	0.35
4	411	6.1	4.4	3.0	1.1	0.7	0.65	2.8	1.2	0.45	0.27
5	406	6.1	4.4	3.1	1.3	0.8	0.85	3.2	1.4	0.52	0.32

TABLE III. Values of Ga-As, As-In, and Ga-P bond lengths in all samples. Also listed is the prediction of the strained-layer model.

Sample	Code	T_1 (ML)	T_2 (ML)	R(Ga-As) (Å)	R(As-In) (Å)	R(Ga-P) (Å)
Model				2.47±0.01	2.60±0.01	2.41±0.01
1	161	10.2	10.2	2.466±0.006	2.60±0.01	
2	384	6.8	6.8	2.477±0.014	2.596±0.007	2.39±0.06
3	380	6.8	6.8	2.475±0.008	2.61±0.01	2.37±0.03
4	411	6.1	4.4	2.49±0.02	2.60±0.01	2.40±0.06
5	406	6.1	4.4	2.47±0.02	2.60±0.01	2.45±0.05

early HRXRD study. However, the experimental CN's are higher than the values predicted by Eqs. 1 and 2; in Table II we list as δ(As-In) and δ(Ga-*P*) the excess of the respective CN's with respect to the abrupt interface values. We conclude that the measured CN's are not compatible with the simple model of a SL with abrupt interfaces, even if we take into account the presence of interface bonds.

Next, we take into consideration the possibility of layers of $InAs_xP_{1-x}$ (at the InP-to-InGaAs interface) and of $In_{0.53}Ga_{0.47}As_{1-y}P_y$ (at the InGaAs-to-InP interface). There is indication from HRXRD and 4 K photoluminescence that such layers are present[9,10,12] and moreover the growth sequence employed suggests their existence; the ability of XAFS to perform a chemically sensitive analysis, which probes in the case of the Ga edge only the second type of interface, adds further evidence and provides a local structural characterization.

Clearly, some simplifying assumptions have to be made in order to analyze the data. Specifically we model the system as composed of four smooth and compositionally homogeneous layers: InP, $InAs_xP_{1-x}$, InGaAs, and $In_{0.53}Ga_{0.47}As_{1-y}P_y$ (in that order). Note that we consider only the possibility of anion intermixing in the strained layers; this simplifying assumption is suggested by the growth sequence that involves only group-V switches. The sum of the thicknesses of InP and $InAs_xP_{1-x}$ is taken to be equal to the nominal InP thickness, T_1, while the sum of the thicknesses of InGaAs and $In_{0.53}Ga_{0.47}As_{1-y}P_y$ is taken to be equal to the nominal InGaAs thickness, T_2. Let n(layer) be the thickness of the particular layer in ML's, let n'(InAsP) be the product of the As concentration x with n(InAsP) and likewise n'(InGaAsP) be the product of the P concentration y with n(InGaAsP); the following relations involving the average As-In and Ga-P CN's, N(As-In), and N(Ga-P), can be obtained (see the Appendix):

$$n'(\text{InGaAsP}) = \frac{T_2 N(\text{Ga-P})}{4}, \tag{3}$$

$$n'(\text{InAsP}) = \frac{[T_2 - n'(\text{InGaAsP})] \times [2.12 - N(\text{As-In})]}{N(\text{As-In}) - 4}. \tag{4}$$

In the above formulas the presence of interface bonds is neglected. The correction to Eqs. 3 and 4 due to interface bonds depends on the value of the concentrations x and y, which are unknown; the maximum value of the correction is -0.5 ML for n'(InGaAsP) and -1 ML for n'(InAsP). In Table II we list values of n'(InAsP) and n'(InGaAsP) obtained by neglecting interface bonds, with the understanding that a possible error of the above magnitude may be present; the quantities obtained are thus useful for a qualitative discussion. The above relations allow to measure directly the product of the concentration with the layer thickness. A lower limit on the concentration can, however, be obtained by noting that the maximum permissible values of n(InAsP) and n(InGaAsP) are T_1 and T_2, respectively; the minimum values of x and y thus obtained are listed in Table II. Likewise, the minimum thicknesses of the interfacial layers are obtained by imposing $x=y=1$ and are thus numerically equal to the values of n'(InAsP) and n'(InGaAsP) listed in Table II; the thicknesses of the strained layers are seen to be a significant fraction of the total period.

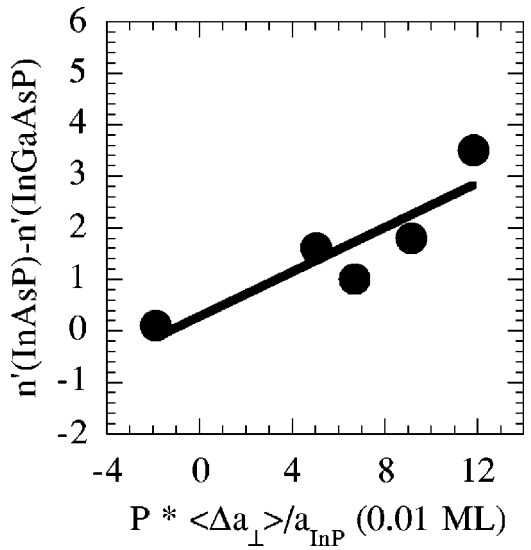

FIG. 5. Plot of n'(InAsP)-n'(InGaAsP) determined from XAFS vs P$\langle \Delta a_\perp / a \rangle$ determined from HRXRD.

It is natural to link the presence of these interfacial layers, which are strained for any value of x or y, to the fact that the average lattice mismatch of the SL is not zero. Specifically, the $InAs_xP_{1-x}$ ($In_{0.53}Ga_{0.47}As_{1-y}P_y$) layers give a positive (negative) contribution to the average perpendicular lattice mismatch $\langle \Delta a_\perp / a \rangle$ for any value of $x(y)$. We can compare the above estimates of n'(InAsP) and n'(InGaAsP) obtained from XAFS to the HRXRD measurements of the average lattice parameter using the following exact relation:

$$P\frac{\langle \Delta a_\perp \rangle}{a} = n'(\text{InAsP})\frac{\Delta a_\perp^{\text{InAs}}}{a} + n'(\text{InGaAsP})\frac{\Delta a_\perp^{\text{InGaP}}}{a}. \tag{5}$$

Here $\Delta a_\perp^{\text{InAs}}/a$ and $\Delta a_\perp^{\text{InGaP}}/a$ are the perpendicular misfits of pseudomorphically strained InAs or InGaP layers on InP. Since the last two quantities are to a good approximation equal in magnitude but opposite in sign a linear relationship between $[n'(\text{InAsP})\text{-}n'(\text{InGaAsP})]$ and $\langle \Delta a_\perp / a \rangle$ is predicted. In Fig. 5 we plot values of n'(InAsP) -n'(InGaP) determined by XAFS as a function of $\langle \Delta a_\perp / a \rangle$ measured by HRXRD, together with a linear fit; the predicted relationship is seen to be obeyed and the slope is, within the errors, equal to the value expected. We conclude that, notwithstanding the simplifying assumptions made, the values of n'(InAsP) and n'(InGaAsP) found from the chemically sensitive XAFS analysis are compatible with the lattice misfits obtained from HRXRD, which is an inherently averaging technique. We note that our analysis finds that the sample with the highest values of n'(InGaAsP) is n. 3, which is reasonable since it is the one grown with longest planarization and switching times; it also exhibits the smallest value of $\langle \Delta a_\perp / a \rangle$, due to the thick quaternary under tensile strain.

We now discuss the value of the bond lengths. While it is generally recognized that due to the stiffness of semiconductor bonds the VCA is violated in bulk pseudobinary alloys,[41–44] the situation in a strained layer has only recently been investigated. In recent publications relative to

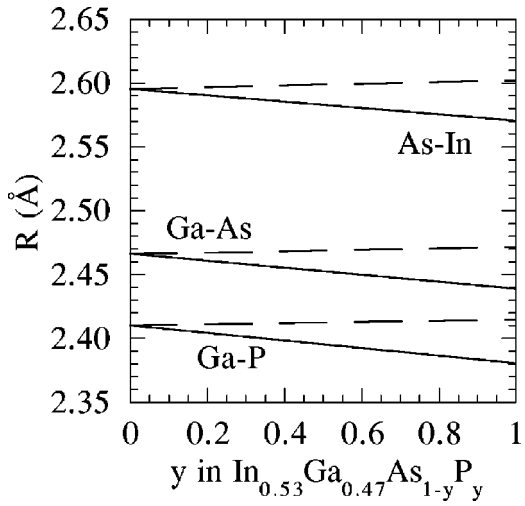

FIG. 6. Predicted values of Ga-P, Ga-As, and As-In bond lengths in bulk (continuous line) and strained (dashed line) $In_{0.53}Ga_{0.47}As_{1-y}P_y$.

$InAs_xP_{1-x}$ (Ref. 26) and $In_xGa_{1-x}As$ strained layers[27,28] we have demonstrated that while the general tendency for semiconductor bonds to be rigid (compared to angles) remains, strain *does* have a measurable effect on the bond lengths: compressive (tensile) strain will compress (stretch) each bond, the constant of proportionality being related to the bond-stretching and bond-bending force constants. The consequence is that bond lengths in strained layers will have different values than in the bulk; for example for $In_xGa_{1-x}As$ it was possible to show that the slope of the bond length versus concentration relation is actually inverted when passing from the bulk to a pseudomorphic layer. The reader should consult Ref. 26 for details on the strained layer model, which we will use in the quantitative analysis of the present data. The value of the bond lengths measured are a weighted average over the whole superlattice structure, which we assume to be composed of four layers repeated several times. As-In bonds are present in the InGaAs, $InAs_xP_{1-x}$, and the $In_{0.53}Ga_{0.47}As_{1-y}P_y$ layers, Ga-As bonds are present in the InGaAs and $In_{0.53}Ga_{0.47}As_{1-y}P_y$ layers, while Ga-P bonds are present only in the quaternary layers. The InGaAs layer is lattice matched to the InP substrate and thus the values of the bond lengths in that layer will be equal to the value in bulk InGaAs, which we take from the literature.[44]

In the two strained layers we use the previously mentioned strained-layer model to predict the value of the As-In, Ga-As, and Ga-P bond lengths. The value of the bond length in a strained ternary layer can be predicted by performing a linear interpolation between two extreme cases: that of negligible tetragonal distortion (in which the values of bond length appropriate for the bulk can be used) and that of a binary-on-binary (in which the symmetry of the systems allows us to use trigonometry to calculate the bond lengths). This model is directly applicable to the $InAs_xP_{1-x}$ layers.[26] For the quaternary layer we have extended the model using a virtual cation $C=\langle In_{0.53}Ga_{0.47}\rangle$. The results of this extension are illustrated in Fig. 6, in which we show the predicted values of the Ga-P, Ga-As, and As-In bond lengths in $In_{0.53}Ga_{0.47}As_{1-y}P_y$, both bulk and pseudomorphic on InP. It is clear from the figure that the three bond lengths are predicted to be essentially constant with the P concentration y. This is due to a compensating mechanism: with increasing y the free lattice parameter tends to decrease (thus inducing a small decrease of bond length) while the tensile stress increases (thus inducing a small increase of bond length); the two effects very nearly cancel each other, resulting in bond lengths that are constant within ~ 0.01 Å. A very similar situation is present in $InAs_xP_{1-x}$ for the As-In bond length, although in this case the bond length in the strained layer is always smaller than in the bulk.

As already stated, the measured value of each bond length will be a weighted average of the value in each layer, making prediction of the final value in principle difficult due to the fact that we do not know thickness and concentrations of each atomic species in all layers. However, the near constancy of each bond length allows us to circumvent this problem eliminating the need to perform an average, provided we accept an indeterminacy of ~ 0.01 Å; we are thus able to predict the value of each bond length, which is listed in Table III.

By inspection of Table III we conclude that the strained-layer model reproduces very well the observed values. We note that the observed near constancy of the bond lengths is thus correctly interpreted as due to the combined (and opposite) effects of strain and free lattice parameter variation. Nearly constant bond lengths imply that any variation of the lattice parameters, including tetragonal distortion, is accommodated at the local scale predominantly by bond-angle distortions rather than by bond-length variation.

Let us finally discuss the impact of our results on simulations of the electronic structure of InGaAs/InP heterostructures. In all simulations, even the most advanced, the VCA is adopted; the question that arises naturally is whether this approximation (which is false from the structural point of view) is adequate or not in reproducing the electronic structure of the system and specifically the BO's. The discussion presented in the work of Peressi *et al.*[8] is useful in this context. In this work, an abrupt interface is assumed and thus the presence of interface layers is neglected. Deviations from the VCA are taken to be a perturbation from the average structure. The conclusion is that deviations from the VCA have a negligible effect on the valence BO to linear order in the perturbation; that is, within linear response theory[45] the VCA is sufficiently accurate. Second-order variations have an effect that is estimated to be of the order of 40 meV. This value is approximately 10% of the total valence BO (~ 350 meV) for this system. In a real heterostructure the situation is more complex due to the presence of strained interface layers, as we have demonstrated. The relevance of our work in this context is therefore to provide an accurate quantitative description of the local structure (in a *real* system with strained interface layers), which can serve as a basis for simulations going beyond the VCA.

ACKNOWLEDGMENTS

We are grateful to M. Peressi for a critical reading of the manuscript. We thank L. Gastaldi for stimulating discussions, G.M. Schiavini for growth of MOCVD samples, and J.F. Bèrar for experimental help on the D2AM beamline. We

acknowledge excellent technical support from F. Campolungo, V. Sciarra, and V. Tullio (INFN-LNF). XAFS and HRXRD measurements were performed at ESRF (BP 220, F-38043 Grenoble CEDEX, France) within the public user program.

APPENDIX: RELATIONS BETWEEN MEASURED COORDINATION NUMBERS AND LAYER THICKNESSES

We wish to show the derivation of Eqs. (1) and (2) for the CN's. Equations (3) and (4) can be derived along the same lines. We take the SL to be composed of an integral number of MLs, each ML being electrically neutral. Each ML is composed of one anion and one cation plane; we use the term ''layer'' to refer to a number of MLs of identical composition (e.g., InP, InGaAs). A cation plane of an InGaAs layer will be indicated as InGa for brevity. It is convenient to distinguish between interface planes (those for which one of the two neighboring planes is not in the same layer) and bulk planes. Given a central atom α and a nearest neighbor β the average CN, $N(\alpha\text{-}\beta)$, is:

$$N(\alpha-\beta)=\frac{\sum_i \mathrm{N}_i(\alpha-\beta)\mathrm{n}_i^{\alpha}}{\sum_i \mathrm{n}_i^{\alpha}}, \tag{A1}$$

where the sum is over all planes, $N_i(\alpha\text{-}\beta)$ is the α-β CN when α is in the ith plane and n_i^{α} is the number of atoms of type α in the ith plane. The thickness of a layer will be indicated as $n(\text{layer})$, in units of ML's. The nominal thicknesses of the InP and InGaAs layers will be indicated as T_1 and T_2, respectively. Consider an ideal InGaAs/InP SL with abrupt interfaces; this is composed of a sequence of planes which we can indicate as $\cdots$In/P/$\langle$InGa$\rangle$/As/$\cdots$/$\langle$InGa$\rangle$/As/In/P$\cdots$. The inverted sequence may also be considered, but this yields identical results. In bulk planes $N(\text{Ga-P})=0$ and $N(\text{As-In})=2.12$. For the Ga-P bonds the only contribution comes from the interface InGa plane; the Ga atoms in this plane are bonded to two P atoms from the neighboring P layer. Considering that Ga atoms are present in all InGaAs layers with identical concentration, application of Eq. (A1) yields:

$$N(\text{Ga-P})=\frac{2}{n(\text{InGaAs})}, \tag{A2}$$

which coincides with Eq. 1 since $T_2=n(\text{InGaAs})$ in the absence of interface layers. As for the As-In bonds we note that in $[n(\text{InGaAs})\text{-}1]$ layers, $N(\text{As-In})=2.12$ (bulk value). In the interface As plane the As atoms are bonded to two In atoms from the neighboring In plane belonging to the InP layer and to 2×0.53 In atoms belonging to the InGa plane in to the InGaAs layer; thus $N(\text{As-In})=2+2\times0.53=3.06$ for the interface As plane. Considering that As atoms are present in all InGaAs layers with identical concentration, application of Eq. (A1) yields:

$$N(\text{As-In})=\frac{2.12\times[n(\text{InGaAs})-1]+3.06}{n(\text{InGaAs})}. \tag{A3}$$

Again, this coincides with Eq. (2) since $T_2=n(\text{InGaAs})$. Equations (3) and (4) can be deduced along the same lines if layers of $\mathrm{InAs}_x\mathrm{P}_{1-x}$ and $\mathrm{In}_{0.53}\mathrm{Ga}_{0.47}\mathrm{As}_{1-y}\mathrm{P}_y$ are introduced between the nominal InGaAs and InP ones.

*Electronic address: Federico.Boscherini@lnf.infn.it
†Present address: ESRF, BP 220, F-38043 Grenoble Cedex, France.

[1] A. Franciosi and C.G. Van de Walle, Surf. Sci. Rep. **25**, 1 (1996).
[2] C.G. Van de Walle and R.M. Martin, Phys. Rev. B **35**, 8154 (1987).
[3] T.Y. Wang and G.B. Stringfellow, J. Appl. Phys. **67**, 344 (1990).
[4] M.S. Hybertsen, Phys. Rev. Lett. **64**, 555 (1990).
[5] J.M. Vandenberg, A.T. Macrander, R.A. Hamm, and M.B. Panish, Phys. Rev. B **44**, 3991 (1991).
[6] L. Nordheim, Ann. Phys. (Leipzig) **9**, 641 (1931).
[7] L. Nordheim, Ann. Phys. (Leipzig) **9**, 606 (1931).
[8] M. Peressi, S. Baroni, A. Baldereschi, and R. Resta, Phys. Rev. B **41**, 12 106 (1990).
[9] A. Antolini, L. Francesio, L. Gastaldi, F. Genova, C. Lamberti, L. Lazzarini, C. Papuzza, C. Rigo, and G. Salviati, J. Cryst. Growth **127**, 189 (1993).
[10] F. Genova, A. Antolini, L. Francesio, L. Gastaldi, C. Lamberti, C. Papuzza, and C. Rigo, J. Cryst. Growth **120**, 333 (1992).
[11] A. Antolini, P.J. Bradley, C. Cacciatore, D. Campi, G. Gastaldi, F. Genova, M. Iori, C. Lamberti, G. Morello, C. Papuzza, and C. Rigo, J. Electron. Mater. **21**, 233 (1993).
[12] C. Lamberti, Comput. Phys. Commun. **93**, 53 (1996).
[13] C. Lamberti, Comput. Phys. Commun. **93**, 82 (1996).
[14] K.J. Beernink, P.K. York, and J.J. Coleman, Appl. Phys. Lett. **55**, 1989 (1989).
[15] A.R. Reisinger, P.S. Zory, and R.G. Waters, IEEE J. Quantum Electron. **23**, 993 (1987).
[16] D. Grutzmacher, J. Cryst. Growth **107**, 520 (1991).
[17] M. Engel, D. Grutmacher, R.K. Bauer, D. Bimberg, and H. Jurgensen, J. Cryst. Growth **93**, 359 (1988).
[18] M. Wataya, N. Sawaky, H. Goto, I. Akasaki, H. Kano, and M. Hashimoto, Jpn. J. Appl. Phys., Part 1 **28**, 1934 (1989).
[19] P.S. Kopev, I.N. Uraltsev, A.L. Efros, D.R. Yakolvev, and A.V. Vinkurova, Sov. Phys. Semicond. **22**, 259 (1988).
[20] K.D. Chik, J. Appl. Phys. **64**, 2138 (1988).
[21] J.P. Landesman, J.C. Garcia, J.C. Massies, G. Jezequel, P. Maurel, J.P. Hirtz, and P. Alnot, J. Vac. Sci. Technol. B **10**, 1761 (1992).
[22] F. Liaci, D. Greco, R. Cingolani, D. Campi, C. Rigo, and D. Soldani, Solid State Commun. **105**, 279 (1998).
[23] C. Rigo, D. Campi, H.C. Neitzert, D. Soldani, L. Lazzarini, and G. Salviati, Mater. Sci. Eng., B **28**, 305 (1994).
[24] C. Lamberti, S. Bordiga, F. Boscherini, S. Pascarelli, G.M. Schiavini, C. Ferrari, L. Lazzarini, and G. Salviati, J. Appl. Phys. **76**, 4581 (1994).
[25] C. Lamberti, S. Bordiga, F. Boscherini, S. Pascarelli, and G.M. Schiavini, Appl. Phys. Lett. **64**, 1430 (1994).
[26] S. Pascarelli, F. Boscherini, C. Lamberti, and S. Mobilio, Phys. Rev. B **56**, 1936 (1997).
[27] F. Romanato, D. DeSalvador, M. Natali, M. Berti, A. Drigo, S. Pascarelli, F. Boscherini, S. Mobilio, G. Rossetto, A. Camporese, G. Torzo, and C. Lamberti, in *ESRF Highlights*, edited by D. Cornuejols (ESRF, Grenoble, 1997) p. 47.

[28] F. Romanato, D.D. Salvador, M. Berti, A. Drigo, M. Natali, M. Tormen, G. Rossetto, S. Pascarelli, F. Boscherini, C. Lamberti, and S. Mobilio, Phys. Rev. B **57**, 14 619 (1998).
[29] C. Lamberti, S. Bordiga, F. Boscherini, S. Mobilio, S. Pascarelli, L. Gastaldi, M. Madella, C. Papuzza, C. Rigo, D. Soldani, C. Ferrari, L. Lazzarini, and G. Salviati, J. Appl. Phys. **83**, 1058 (1998).
[30] R. Shioda, H. Oyanagi, Y. Kuwahara, Y. Takeda, K. Haga, and H. Kamei, Jpn. J. Appl. Phys., Part 1 **33**, 5623 (1994).
[31] Y. Kuwahara, H. Oyanagi, R. Shioda, Y. Takeda, H. Yamaguchi, and M. Aono, Jpn. J. Appl. Phys., Part 1 **33**, 5631 (1994).
[32] M.G. Proietti, S. Turchini, J. Garcia, G. Lamble, F. Martelli, and T. Prosperi, J. Appl. Phys. **78**, 6574 (1995).
[33] M.G. Proietti, S. Turchini, F. Martelli, J. Garcia, and T. Prosperi, J. Appl. Phys. **77**, 62 (1995).
[34] J.C. Woicik, J.G. Pellegrino, B. Steiner, K.E. Miyano, S.G. Bompadre, L.B. Sorensen, T.-L. Lee, and S. Khalid, Phys. Rev. Lett. **79**, 5026 (1997).
[35] J.C. Woicik, C.E. Bouldin, K.E. Miyano, and C.A. King, Phys. Rev. B **55**, 15 386 (1997).
[36] A. Mircea, R. Mellet, B. Rose, P. Dastè, and G.M. Schiavini, J. Cryst. Growth **77**, 340 (1986).
[37] C. Lamberti, G. Gastaldi, F. Boscherini, and S. Pascarelli (unpublished).
[38] S. Pascarelli, F. Boscherini, F. D'Acapito, J. Hrdy, C. Meneghini, and S. Mobilio, J. Synchrotron Radiat. **3**, 147 (1996).
[39] P.A. Lee, P.H. Citrin, P. Eisenberger, and B.M. Kincaid, Rev. Mod. Phys. **53**, 769 (1981).
[40] A. Michalowicz, J. Phys. IV **7-C2**, 325 (1997).
[41] J.C. Mikkelsen and J.B. Boyce, Phys. Rev. Lett. **49**, 1412 (1982).
[42] J.C. Mikkelsen and J.B. Boyce, Phys. Rev. B **28**, 7130 (1983).
[43] Y. Cai and M.F. Thorpe, Phys. Rev. B **46**, 15 872 (1992).
[44] Y. Cai and M.F. Thorpe, Phys. Rev. B **46**, 15 879 (1992).
[45] A. Baldereschi, M. Peressi, S. Baroni, and R. Resta, in *Semiconductor Superlattices and Interfaces*, Proceedings of the International School of Physics ''E. Fermi,'' Course CXVII, edited by L. Miglio and A. Stella (Academic Press, New York, 1993), p. 59.